FISEVIER

Contents lists available at ScienceDirect

Construction and Building Materials

journal homepage: www.elsevier.com/locate/conbuildmat





Cross-laminated strand veneer lumber mass timber panels from thermally modified strands

Ruben Jerves a,b,*, Vikram Yadama a,b, Matthew Aro c, Manuel Raul Pelaez-Samaniego b,d

- ^a Department of Civil and Environmental Engineering, Washington State University, Pullman, WA 99164, USA
- ^b Composite Materials and Engineering Center, Washington State University, Pullman, WA 99164, USA
- ^c Natural Resources Research Institute, University of Minnesota Duluth, Duluth, MN 55811, USA
- d Department of Applied Chemistry and Systems of Production, Faculty of Chemical Sciences, Universidad de Cuenca, Cuenca, Ecuador

ARTICLE INFO

Keywords: Wood-strands Mechanical properties Physical properties Laminate mechanics Thermal modification

ABSTRACT

Thin-strand composite panels and subsequent mass timber beams were produced using thermally modified wood strands in a pressurized system. The effects of thermal modification (TM) temperature and dwell time on the mechanical, moisture, and decay performance of panels were studied. TM reduced moisture sorption and increased decay resistance. The thin-strand composites were evaluated in flexure and benchmarked against commercially available structural products. Moreover, the mass timber beams' out-of-plane bending was accurately predicted with traditionally used laminated beam theory. The study shows that TM, under controlled conditions, enables the production of high-performing wood-strand panels with improved dimensional stability and decay resistance.

1. Introduction

Mass timber construction is rapidly growing in North America, mostly due to wood's renewability, versatility, abundance, and good mechanical performance. Mass timber is often described as large structural panels made by assembling layers of dimensional lumber together with either glue, nails, or dowels; in many cases, with the grain of alternate layers orthogonal to each other, such as cross-laminated timber (CLT). However, layers in mass timber panels are not always dimensional lumber but could also consist of structural composite lumber (e.g., LSL, OSL, or LVL), which is the case in this study. In contrast to other construction materials (e.g., concrete and steel), wood has a high strength-to-weight ratio and fewer environmental impacts, with the added benefit that it is renewable and, if adequately managed, also sustainable. Mass timber construction offers relatively short construction times and improves building quality with minimal material waste, since the elements are prefabricated off-site in a controlled setting. Despite the recognized benefits of using mass timber for construction, wood's durability and dimensional stability with changing environmental conditions is of concern and needs to be addressed for the continued advancement of mass timber construction. Extreme care is required by builders to protect wood members from exposure to high moisture environments to ensure long-term durability.

Currently, mass timber products are fabricated mostly from highquality lumber, which requires long growing times and strict quality control processes, which increases the cost of the end-products [1]. Conversely, small-diameter timber (SDT), widely available in North America and other regions, has not received the same attention for mass timber production, primarily because of its lower wood quality since it contains more juvenile wood, which inherently has greater variability in mechanical properties and lower dimensional stability as compared to mature wood [2,3]. The value-added use of SDT could improve the economic competitiveness of the forest industry and help mitigate forest fires [4], often prominent in regions with dense stands of SDT. Moreover, removing SDT from forests allows for a more diverse forest structure while providing healthier wildlife habitat and protecting watersheds [4]. Potential uses of SDT that have been explored include CLT [5] and other engineered wood products [6], direct use for affordable housing construction [7,8], and wood posts in highway applications [9]. Nevertheless, SDT has relatively high harvest and processing costs and yields low quality products. Thus, more work is required to identify pathways for efficient uses for low-value SDT material collected from forest thinning operations, with the long-term goal of reducing wildfires [10] and managing our forests more sustainably.

Any methods for adding value to SDT should improve the quality of the feedstock (e.g., durability and dimensional stability) and the resulting products. One such method is thermal modification (TM), which in timber is commonly referred to as thermally modified timber (TMT), but for the scope of this work the more general case of TM is used

^{*} Corresponding author at: Department of Civil and Environmental Engineering, Washington State University, Pullman, WA 99164, USA. E-mail address: ruben.jerves@wsu.edu (R. Jerves).

henceforth. TM is widely recognized by the forest products industry as a method to improve the dimensional stability and fungal decay resistance of wood. In recent years, there has been a growing interest in using TM processes conducted at high-temperatures and under inert environments to achieve the desired improvements of moisture and rot resistance [11-17]. However, the effects of TM are influenced by many variables, both in the wood itself and the TM process. Wood species, starting wood quality (e.g., presence of checks and cracks), wood thickness, and initial wood moisture can impact the quality of the TM in wood. Likewise, the TM process conditions such as dwell time, temperature, rate of heating and cooling, process atmosphere, and pressures also impact the quality of the thermally modified wood [18]. Therefore, it is critical to understand the impacts of these variables for successful TM of wood, especially of SDT due to its high amount of juvenile wood, as well as to effectively scale up the process and commercialize thermally modified composite wood products.

TM of wood and wood products covers a wide range of technologies [18]. In contrast to chemical modification, TM uses heat instead of chemicals, and is carried out either in dry or wet environments [19]. TM in wet environments requires the use of water (or steam), which can be condensed at the end of the treatment and potentially used for energy recovery or other products (e.g., organic chemicals, biofuels). Dry treatments, on the other hand, can use air or an inert environment [19]. In both cases, TM reduces wood water affinity, which results in improved dimensional stability and fungal decay resistance. Nevertheless, TM negatively impacts mechanical properties of wood, although in some cases a slight increase in stiffness has been reported [20-25]. The reasons for the physical, chemical, and structural changes occurring in wood during TM processing have largely been studied. According to Shafizadeh and Chin [26], hemicelluloses are more easily degraded than the other wood structural components (i.e., cellulose and lignin) during thermal treatment. Hillis [27] noted that the reduction of hemicelluloses provides hygroscopicity to wood and that TM of wood under moist environments could lead to higher dimensional stability. Hemicelluloses are highly hydrophilic and, thus, their extraction is desirable for decreasing water absorption of wood [28]. When wood is heated at or above 140 °C, it undergoes a dehydration process, where hydroxyl (-OH) groups, which attract moisture, are progressively lost as temperature increases [18]. Mitchell [29], referred by Hill [18], observed that the use of moist environments during TM accelerates the formation of organic acids, which catalyzes the hydrolysis of hemicellulose and, at lesser extent, of amorphous cellulose, with amorphous cellulose attracting more water than crystalline cellulose due to its large content of free -OH groups [30]. Ding [31] also noted that pressurized steam further accelerates the degradation of amorphous cellulose. After TM, wood decay resistance is expected to be improved due to the degradation of polysaccharides, which serves as an alimentary source for wood-rotting fungi, as well as due to other possible changes in the chemical composition of the modified wood [32,33]. Another prospective cause of the improved fungal decay resistance is linked to the reduced moisture content (MC) of the cell wall [18]. It is thought that the loss of -OH groups affects the ability of enzymes to metabolize the wood substrate. The referred works provide evidence that water or steam used in TM removes hemicelluloses from wood, which benefits wood decay resistance and reduces its water sorption capacity. However, during TM, reduction of hemicelluloses can also decrease the mechanical properties of the end-product. Modulus of rupture (MOR) (i.e., bending strength) can decrease at higher treatment temperatures [13,34–36]. Modulus of elasticity (MOE) (i.e., stiffness), conversely, may not change significantly or even increase slightly, depending on treatment intensity.

Many studies have also been performed on the effects of TM on wood strands/particles before the fabrication of wood composites [37–40]. In these, different types of TM have been conducted, such as hot water extraction, dry and steamed environments, and pressurized (closed) and non-pressurized (open) process. Results from these also

indicate improvements in dimensional stability and changes in mechanical properties, reporting reduction or improvement. In this work, we go a step further by fabricating and characterizing the behavior of mass timber panels, namely cross-laminated strand veneer lumber (CLSVL), from thin strand veneers produced from thermally modified wood strands. In this case, the TM process used consists of a pressurized system, expected to increase the degradation of hemicelluloses and sugars in wood, likely due to a combination of better heat transfer, reduced evaporative cooling, accumulation of thermal degradation products, and presence of water in the wood [41,42]. Moreover, the composite material manufacturing process implements a technology developed by Weight and Yadama [43,44] that uses thin strands in the manufacturing of veneers to obtain a uniform vertical density profile in the composite, resulting in improved mechanical performance of the veneers later used in the production of the CLSVL. Hence, the proposed project provides a potential solution to address the dimensional stability and degradation issues due to moisture infiltration and accumulation in mass timber panels with the benefit of adding value to underutilized SDT. In order to achieve this, the TM process should be designed to promote fungal decay resistance, improve dimensional stability, and reduce water sorption, all without significantly altering the wood's mechanical properties and imparting brittleness to the end product. Thus, the objective of this work was twofold: (a) to investigate the effects of TM of wood strands and subsequent wood strand composite panels and (b) assess the out-of-plane bending performance of CLSVL mass timber panels manufactured from thin veneers produced from thermally modified wood strands.

2. Materials and methods

Fig. 1 shows the steps followed to conduct the work and the following sections describe each operation.

2.1. Strand's processing and thermal modification

Lumber from small diameter Engelmann spruce (*Picea engelmannii*) and lodgepole pine (*Pinus contorta*), classified as ESLP, were obtained from Idaho Forest Group, with the mix predominantly consisting of lodgepole pine. Before stranding, the SDT lumber was cut into $\sim\!150$ mm slats that were soaked in water for approximately 48 h to reach a moisture content (MC) close to 40% to help the stranding process. Strands were then produced from the wet slats using a CAE disc-strander rotating at 500 rpm. The nominal dimensions of the strands were 148.0 mm \times 19.3 mm \times 0.38 mm (length \times width \times thickness). The strands were then air dried at room conditions until the MC was between 7 and 10% prior to thermal modification.

For the thermal modification process, four sample groups of ~10 kg each were randomly selected from the air-dried strands and subjected to TM at three different temperatures: 150 °C, 165 °C, 180 °C and dwelling times of 45, 90, 135, and 180 min for each treatment temperature. The TM was conducted at the University of Minnesota, Duluth - Natural Resources Research Institute, using a 0.5 m³ IWT/Moldrup autoclave. For each TM, 4.5 kg of the strands were placed in two stainless steel mesh baskets with a stainless-steel cover sheet placed on top of the baskets to protect the strands from excess water spray during the cooling cycles. At the beginning of each cycle, a fine water mist was sprayed into the autoclave for 3 min to allow for pressure buildup; approximately 0.4 gallons of water was inputted. During each TM cycle, the steam pressure and temperature was monitored and recorded. After the strands remained at the desired temperature for a given dwell time, the cooling process used an automated fine water spray inside the autoclave. Fig. 2 shows a typical TM process routine where the heating step is indicated in phase I and II, the holding (dwell time) step in phase III, and the cooling step in phases IV, V, and VI. After the TM process, the strands were dried in a convection oven at 103 °C +/- 2 °C for 24 h and the mass loss was calculated. The TM conditions for each treatment group are shown in Table 1.

Table 1
Thermal modification conditions.

Peak temperature	Dwell time	Total time	Initial wood MC	Peak pressure	Weight-loss
150 °C	180 min	13 h 6 m		0.32 MPa	1.13%
	45 min	14 h 22 m		0.44 MPa	not determined
165 °C	90 min	15 h 51 m	8%	0.44 MPa	not determined
	135 min	16 h 12 m	070	0.45 MPa	not determined
	180 min	17 h 23 m		0.44 MPa	4.94%
180 °C	180 min	19 h 44 m		0.48 MPa	11.50%

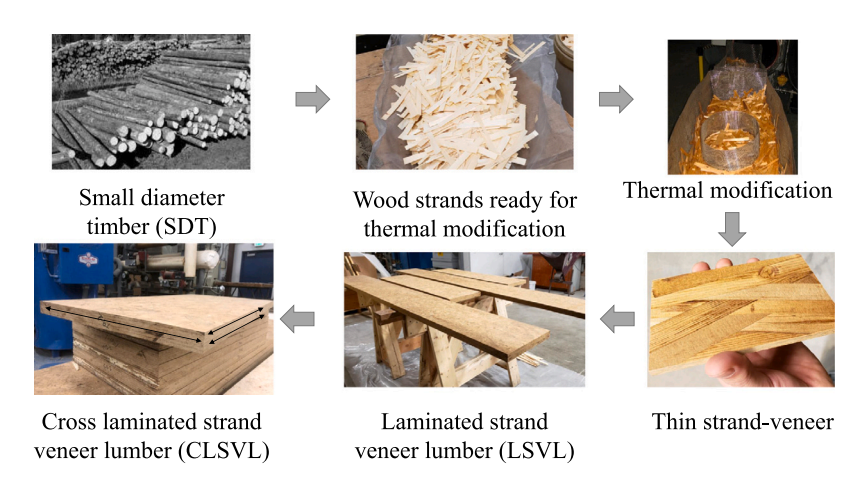


Fig. 1. Process followed for conducting the work: from small diameter timber to cross-laminated strand veneer lumber.

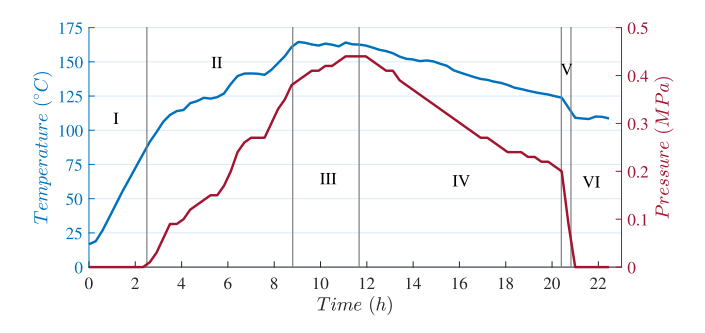


Fig. 2. TM temperature and pressure profile for 165 °C, 180 min dwell time cycle.

2.2. Characterization of thermally modified strands

2.2.1. Tensile properties

Young's modulus (E) and ultimate tensile strength (UTS) of the thermally modified and control (i.e., strands not subjected to TM) wood-strands were determined via tensile tests parallel to the grain. Since no specific standard exists for testing wood-strands in tension, guidelines were followed as per Kohan [45] regarding specimen's geometry and Jeong et al. [46] concerning loading rate. A total of 30 specimens per treatment type were tested. Specimens were selected to guarantee uniform width and relatively straight grain or low deviation in grain with respect to the longitudinal axis of the strands. Before testing, the wood-strands were conditioned at 22 °C and a relative humidity (RH) of 65%. The specimen dimensions were measured with an accuracy of 0.025 mm and weighed to an accuracy of 0.01 g. MC of all specimens was measured as per ASTM D4442-16. Mechanical testing was performed with an Instron load frame equipped with an 8.89 kN load cell at a loading rate of 0.254 mm/min, and the longitudinal strain was recorded using an Epsilon extensometer with a gauge length of 12.7 mm, Model 3442-0050-010-ST. Wedge action tensile grips were used throughout the test. The density of each specimen was determined and used to account for the effects it may have on the tensile properties.

2.2.2. Surface tension and wettability

Surface properties of the thermally modified and control wood-strands were determined using contact angle measurements [47–51]. Contact angle values were used as an indirect method to compute surface free energy (*SFE*) and assess wettability of p-MDI resin (used in this study to hot-press wood strand composite panels, see Section 2.3) by means of penetration and spreading rate. A VCA Optima video contact angle analyzer was used to measure advancing contact angle via sessile drop method. *SFE* was computed using the Fowkes method, Eqs. (1) and (2) [52–54], based on Young's equation [55].

$$\gamma_s^d = 0.25 \gamma_L^d (1 + \cos \theta)^2 \tag{1}$$

$$\gamma_s^p = \frac{\left[0.5\gamma_l \left(1 + \cos\theta\right) - \left(\gamma_s^d \gamma_l^d\right)^{0.5}\right]^2}{\gamma_s^p} \tag{2}$$

The testing liquids used were distilled water (polar dominant component) and diiodomethane from Sigma-Aldrich, 99% assay (dispersion dominant component). A total of three droplets per testing liquid were used for each type of TM and control group, in triplicates in all cases. The contact angle was measured with liquid spreading along the grain direction at a time t = 1 s (time after the drop was placed on the solid surface). The droplet dosage was 3 μl for the distilled water and 0.75 μl for the diiodomethane. This dosage was based on the maximum amount of liquid that would form a droplet big enough to barely remain at the tip of the syringe to be then picked up by the wood-strand. For the SFE determination, the contact angle θ was taken from the average of the right and left contact angle of the droplet. Moreover, the penetration and spreading rate of p-MDI resin was determined by means of a dynamic wettability model proposed by Shi and Gardner, Eq. (3) [48], frequently adopted to study wettability in wood [50,56-58]. In the equation, θ_i is the initial contact angle (°), θ_e is the equilibrium contact angle (°), t represents wetting time (s), and K is a constant indicating the spread and penetration rate of the liquid into the porous structure of wood (1/s). Measurements were performed along the grain direction with a droplet volume of 6 ml. The contact angle was measured at a rate of 4 points/second for at least 80 s, assuring to reach the equilibrium contact angle, referred as the minimum angle the droplet forms with the solid substrate. The experimental values were then fitted to the Shi-Gardner model using the Levenberg–Marquardt algorithm [59] by varying the parameter K for each measurement. A total of three droplets per specimen were tested, with two specimens for each treatment type.

$$\frac{\mathrm{d}\theta}{\mathrm{d}t} = K\theta \left(\frac{\theta_e - \theta}{\theta_i - \theta_a} \right) \tag{3}$$

2.2.3. Moisture sorption

Water sorption was determined for the thermally modified and control wood-strands through moisture sorption isotherms at 22 $^{\circ}$ C with a total of seven randomly selected strands per each TM and control group, using a conditioning chamber Russells Elite G-series. The equilibrium moisture content (EMC) was recorded for each specimen for a RH ranging from 20% to 95% and was then used to build the adsorption curves. All weights were recorded with a precision of 0.001 g. At the end of testing, the dry weight of the strands was determined as per ASTM D4442-16 using the oven-dry method. The experimental data was fitted to the three parameter Guggenheim–Anderson–deBoer (GAB) model [60–63], Eq. (4), to understand the sorption physics.

$$EMC = M_m \cdot \frac{K_{GAB} \cdot C_{GAB} \cdot RH}{\left(1 - K_{GAB} \cdot RH\right) \cdot \left(1 - K_{GAB} \cdot RH + C_{GAB} \cdot K_{GAB} \cdot RH\right)} \tag{4}$$

Where, M_m , C, and K_{GAB} (the fitted parameters) refer to the monolayer water capacity (%), equilibrium constant related to the monolayer sorption, and the equilibrium constant related to the multilayer sorption, respectively. The model coefficients were found using the Levenberg–Marquardt algorithm [59].

2.2.4. Degree of crystallinity

X-ray diffraction (XRD) was used to estimate the degree of crystallinity using the Segal method [64], Eq. (5). Here, C_rI represents the degree of crystallinity, I_{002} the intensity peak corresponding to the plane in the sample with Miller index 002 found at $2\theta \approx 22^\circ$ (a.u.), and I_{am} the intensity of diffraction of the amorphous region found at $2\theta \approx 18.5^\circ$ (a.u.). Before XRD, the wood-strands were ground using a Thomas milling grinder and passed through a 60-mesh sieve. XRD measurements were performed using a Rigaku Miniflex600 with a CuK α radiation ($\lambda = 1.541$ Å) operating at 40 KV and 15 mA. The $2\theta/\theta$ angle was measured in a range from 5° to 45° at a rate of 0.05°/s. Four powder samples were prepared and scanned for each treatment condition

$$C_r I(\%) = \frac{I_{002} - I_{am}}{I_{002}} \times 100 \tag{5}$$

2.2.5. Chemical composition

Two samples of 5 grams (ground, 60-mesh sieved) of known MC per each treatment group were soxhlet extracted with CH_2Cl_2 (150 mL) for 22 h to remove extractives following ASTM D1108. Furthermore, these samples were analyzed in triplicate to determine chemical composition (i.e., sugars and lignin).

2.3. Manufacture of wood-strand composite panels

Panels from wood strands were hot pressed using a hydraulic press with plate dimensions of 889 \times 889 mm, controlled by Pressman control system software. Before pressing, all the wood-strands were conditioned at 70% RH and 20 °C. Polymeric diphenylmethane diisocyanate (pMDI) resin was spray-blended onto the wood-strands in a rotating drum, ensuring a uniform application. The resin content used was 4.5% by weight of dry wood strands. The strands were then handformed into a forming box, which consists of a wood frame with vanes separated by 76.2 mm, to obtain a theoretical preferred orientation of the strands of $\sim \pm 30^\circ$ with respect to the longitudinal direction of the panel. Once the mat was fully formed, it was hot-pressed at 140 °C

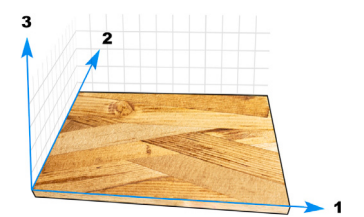


Fig. 3. Definition of local coordinates of a wood-strand composite panel.

for a total curing time of 360 s to a target thickness of 6.35 mm and density of 640 kg/m^3 . Afterwards, the panels were edge trimmed and cut accordingly to prepare test specimens. The type of specimens and respective dimensions, as well as the sample size for each panel, are presented in Figure 15 and Table 6, respectively.

2.4. Performance of wood-strand composite panels

2.4.1. Mechanical properties

The wood-strand composite panels local coordinates (1, 2, and 3), where axis 1 is parallel to the wood fiber (longitudinal direction) and axes 2 and 3 are orthogonal to 1 are shown in Fig. 3.

A three-point bending test was used to evaluate the mechanical properties of the wood-strand composite panels along local directions 1 and 2 to determine the moduli of elasticity in bending (E_1 and E_2) and the out-of-plane shear moduli (G_{13} and G_{23}). To estimate the material properties, the bending specimens were tested at multiple span-to-depth ratios (20, 8.5, 6.5, and 5.5), similar to the procedure established in ASTM D198-Appendix X4, with a linear regression between $x = (d/l)^2$ and $y = (1/E_{app})$ defined by Eq. (6).

$$\frac{1}{E_{app}} = \frac{1}{E_{sh}} + \frac{1}{kG} \left(\frac{d}{l}\right)^2 \tag{6}$$

Where k represents the shape factor, E_{app} the apparent modulus of elasticity, E_{sh} the shear free modulus of elasticity, G the shear modulus, and d and l the panel thickness and the span, respectively. Furthermore, the bending modulus of rupture (MOR) along the local direction 1 was also determined from a three-point-bending test following ASTM D1037. After testing, the MC of the samples was measured as per ASTM D4442-16 and the corresponding densities were computed and used to account for the effects it may have on the elastic constants and MOR along the direction 1.

2.4.2. Internal bond

Internal bond (IB) strength of the wood-strand composite panels was used as a method to evaluate bond performance between the strands for different TM conditions. The test was carried out as per ASTM D1037-12. Mean estimates from X-ray vertical density profile (VDP) for each specimen were used to account for the effects that density may have on IB

2.4.3. Water absorption and thickness swelling

A water absorption and thickness swelling (WA and TS) test was conducted following ASTM D1037-12 to study the effect of TM on moisture uptake and to indirectly infer changes in dimensional stability. Measurements of WA and TS were taken for each specimen 24 h after submersion in water at a temperature of 20 \pm 1 °C. After testing, the MC of the specimens was measured as per ASTM D4442-16.

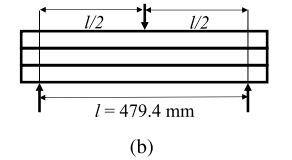


Fig. 4. Out-of-plane-bending test layout for (a) four-point and (b) three-point bending.

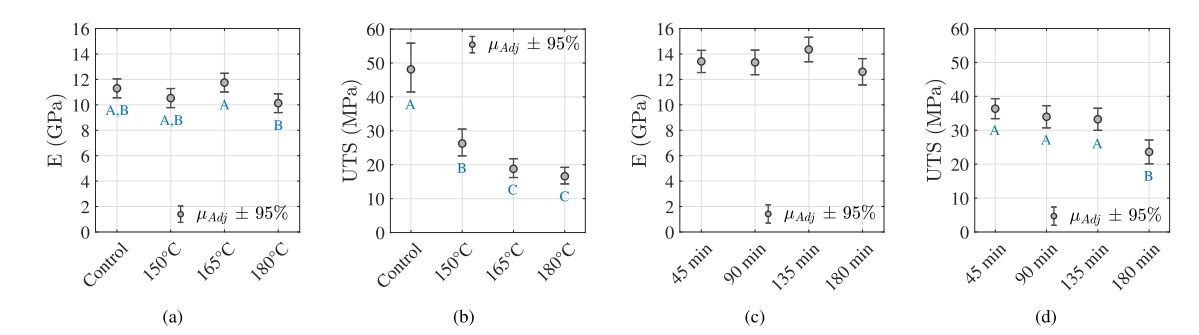


Fig. 5. Effects of TM on tensile properties (E and UTS) of wood-strands: (a) and (b) temperature effect with dwell time of 180 min, (c) and (d) effect of dwell time at working temperature of 165 °C. Groups with the same letter are not significantly different (p-value < 0.05).

2.5. Decay resistance of wood-strands and wood-strand composite panels

The different types of thermally modified wood-strands and manufactured panels were tested for their resistance to decay following AWPA E10-16 by laboratory soil-block cultures. Wood-strand specimens and panel specimens were exposed to the brown rot fungus *G. trabeum*, a prevalent fungi among softwoods species, for 39 days and 55 days, respectively. For the test, the wood-strands were cut to 90 \times 19 mm (with original thickness of 0.38 mm) and the panels were cut into $12.5 \times 12.5 \times 6.4$ mm specimens before the exposure to fungi. For comparison purposes, untreated and alkaline copper quaternary (ACQ)-treated Southern yellow pine specimens were prepared and exposed to the same conditions. A total of five replicates were tested for each treatment type for both wood-strands and panels.

2.6. Statistical analysis of strands characterization and panels performance

All statistical analyses were performed with SAS software using a generalized linear model. For the mechanical properties, the effects of the density of each specimen were considered as a covariate. Furthermore, pairwise Tukey's multiple comparison procedure was used to compare significantly different groups across different analyses. All ANOVA results and validations of model assumptions are presented in Table 7.

2.7. Out-of-plane flexural performance of cross-laminated strand veneer lumber (CLSVL)

2.7.1. Experimental design and manufacture of CLSVL

The out-of-plane bending shear performance of CLSVL made of control and thermally modified wood-strands was evaluated. Two different shear type failure bending specimens were prepared with different span-to-depth ratios, 1/h, and different loading configurations. For instance, a beam with 1/h ≥ 20 tested under four-point bending with equivalent concentrated loads symmetrically applied (Fig. 4(a)), and another beam with 1/h ≤ 5 loaded at mid-span (Fig. 4(b)). In the four-point bending test, the neutral axis's mid-span deflection was measured using a string pot with a 250 mm stroke held in a U-shaped yoke suspended on two nails placed on the neutral axis at both reaction points. For the three-point bending test, the mid-span deflection was recorded with a 25.4 mm stroke linear variable differential transducer (LVDT).

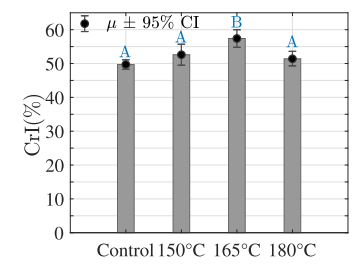


Fig. 6. Temperature effects on degree of crystallinity at 180 min dwell time. Groups with the same letter are not significantly different (p-value < 0.05).

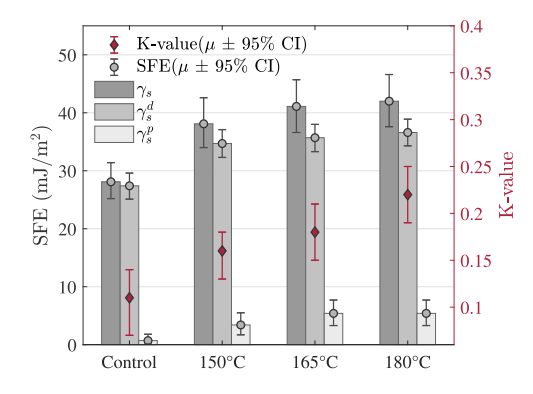


Fig. 7. Effect of temperature on surface free energy and pMDI resin dynamic wettability (K-value from the Shi-Gardner model) for TM at 180 min dwell time.

Due to limited availability of thermally modified material and after finding that the 165 °C/180 min treatment showed the best overall performance (i.e., mechanical properties, moisture resistance, and decay resistance), only this type of thermally modified wood-strands were used for the manufacture and study of CLSVL. For the fabrication of the CLSVL beams, a total of ten 2440 \times 1220 \times 7.62 mm wood-strand panels were hot-pressed using a hydraulic hot press with plate dimensions of 2642 \times 1372 mm, following the procedure described in Section 2.3. Five panels were manufactured using control strands and five using the thermally modified strands (165 °C/180 min). The wood-strands were first conditioned at 16 °C and 75% RH. Immediately prior to the application of pMDI resin, the wood-strands were

Structural Carbohydrates and Lignin

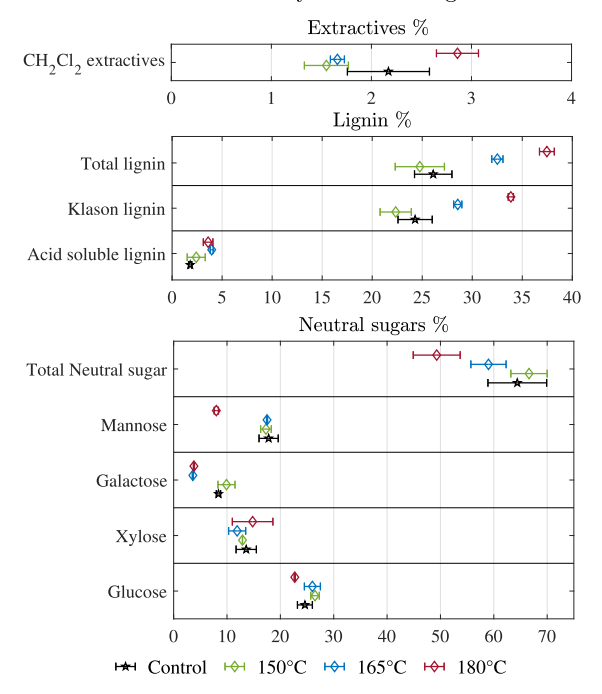


Fig. 8. Structural carbohydrates and lignin content changes in strands treated at different temperatures and 180 min dwell time.

uniformly sprayed with water to reach a MC \sim 12% in a rotating drum. After pressing, the panels were trimmed and cut to specific sizes to manufacture a total of four 15-ply CLSVL beams: two with dimensions $2438 \times 305 \times 95$ mm (length \times width \times thickness), one from control strands and the other from the thermally modified strands, and two beams with dimensions $610 \times 305 \times 95$ mm (length \times width \times thickness), one control and one from thermally modified strands. The 15-ply CLSVLs were cross laminated, i.e., the outer five plies oriented along the longitudinal direction or axis 1 (See Fig. 3) and the five core plies oriented along the transverse direction or axis 2 and orthogonal to the outer plies. Strand plies were coated with polyurethane resin (PUR) Henkel HBX 602 (hand rolled at a rate of 0.17 g/m2 within each laminate with an assembly time less than 60 min) and cold pressed at a target pressure of 120 psi into CLSVL for 180 min, as established by the resin manufacturer. After trimming and sanding to assure a uniform thickness among the beams, with a tolerance of ~ 0.2 mm, the beams were conditioned at 16 °C and 75% RH.

2.7.2. Modeling of CLSVL

Although the out-of-plane bending behavior of similar mass timber products such as cross-laminated timber (CLT) is well understood, there is a need to apply laminated beam theory, a mechanics-based approach commonly applied in composites to predict its flexural behavior, and validate it for CLSVL, considering two major differences when compared to traditional CLT: geometry and material. Geometry changes involve the use of different thickness-to-width ratios of each ply, and material changes are related to the use of thermally modified strands. For modeling CLSVL, two steps were considered: (1) The Shear Analogy Method (SAM) described in the CLT Handbook and other works [65,66] was implemented to compute effective section properties of the beam element so that deflections could be estimated. This method accounts for the effects of shear deflections derived from the Timoshenko beam theory (TBT) and, separately, the pure flexural deflections derived from Euler-Bernoulli beam theory (BBT). From the SAM method, the effective bending stiffness $(EI)_{eff}$ is derived, which results in Eq. (7).

Table 2

Contact angle of different testing liquids on strands treated at 180 min dwell time (letter grouping indicates the results from comparison of means at an alpha-level of 0.05).

Contact a	Contact angle [°]								
	Distille	d water		Diiodo	omethane				
	μ	SD	Letter grouping	μ	SD	Letter grouping			
Control	119.5	(6.6)	A	62.1	(4.6)	A			
150 °C	127.4	(8.4)	AB	49.2	(10.3)	В			
165 °C	133.5	(7.6)	В	47.4	(6.5)	В			
180 °C	132.7	(11.1)	В	45.7	(3.5)	В			

Table 3GAB parameters for thermally modified wood-strands.

Temperature	Dwell time	M_m	K_{GAB}	R_{adj}^2
Control		0.049	0.787	0.969
150 °C	180 min	0.047	0.755	0.925
165 °C	45 min	0.036	0.732	0.821
165 °C	90 min	0.034	0.739	0.891
165 °C	135 min	0.035	0.730	0.883
165 °C	180 min	0.032	0.678	0.777
180 °C	180 min	0.044	0.681	0.897

Likewise, the out-of-plane effective shear stiffness $(GA)_{eff}$ is computed using Eq. (8).

$$(EI)_{eff} = \sum_{i=1}^{n} E_i b_i \frac{h_i^3}{12} + \sum_{i=1}^{n} E_i A_i z_i^2$$
 (7)

$$(GA)_{eff} = \alpha^2 \left[\frac{h_1}{2G_1b_1} + \sum_{i=2}^{n-1} \frac{h_i}{G_ib_i} + \frac{h_n}{2G_nb_n} \right]^{-1}$$
 (8)

In Eqs. (7) and (8), E_i is the modulus of elasticity; b_i and h_i are the width and thickness of each lamina or ply, respectively; A_i is the cross-sectional area of the ith lamina; z_i is the distance from the centroid of the ith lamina to the centroid of the beam's cross section; G_i is the shear modulus for the ith laminate; and α is the distance between the centroids of the lower and upper layers or plies. (2) To estimate the normal and shear stress distribution across the cross section of the CLSVL elements, the equivalent transform section method [67] was used

3. Results and discussion

3.1. Mechanical, physical, and chemical effects on wood-strands from the thermal modification

Results from the tensile tests of strands are shown in Fig. 5. Overall, TM at 150 °C and 180 °C for 180 min does not affect E as compared to the control (at 95% level of confidence), and although not statistically significant, there was a slight increase in E for strands thermally modified at 165 °C/180 min. Likewise, E values are unaffected by dwell time during TM, with an apparent increase up to a temperature of 165 °C and a decrease at a temperature of 180 °C, despite these not being statistically significant, as shown in Fig. 5(c). Moreover, there is a negative impact on UTS of strands with different levels of TM temperature with a constant dwell time of 180 min, as shown in Fig. 5(b). Fig. 5(d) shows that the dwell time for strands thermally modified at 165 °C does not have a significant effect on the tensile strength, except for the 180 min treatment, which has lower UTS values. Similar results on strength and modulus of elasticity of lumber and wood composites after TM have been reported previously [24,37,68,69]. For instance, Esteves and Pereira [24] and Sandberg and Kutnar [69] described that E values of wood had an initial increase with TM and a subsequent drop as TM conditions intensified, especially for the case of softwood species. The authors also pointed out that strength was progressively diminished

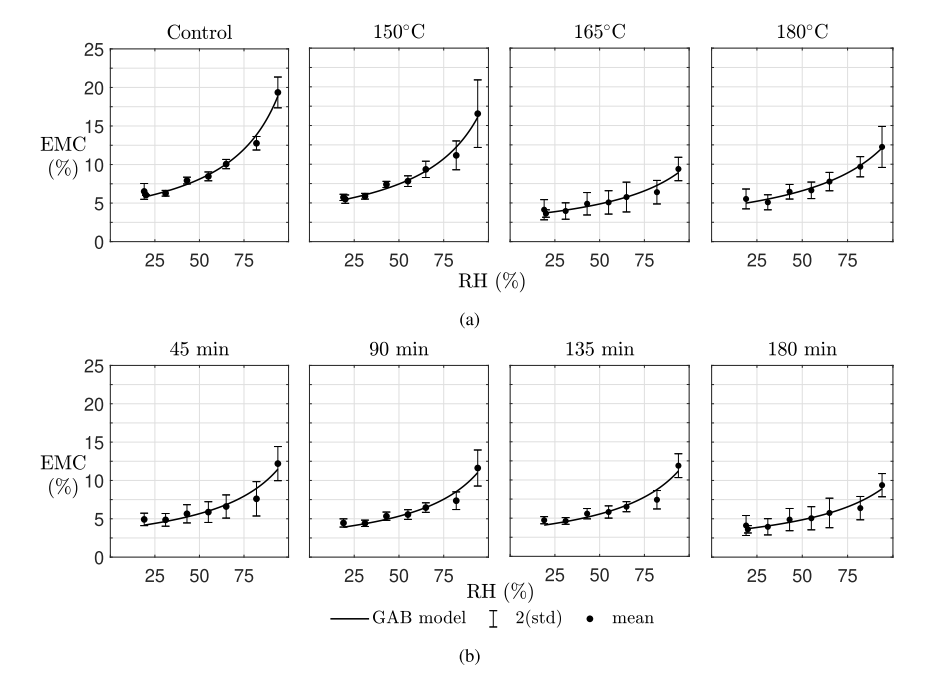


Fig. 9. TM influence on moisture sorption isotherms at 22 ±°C: (a) temperature effects at 180 min dwell time, (b) dwell time effects at 165 °C.

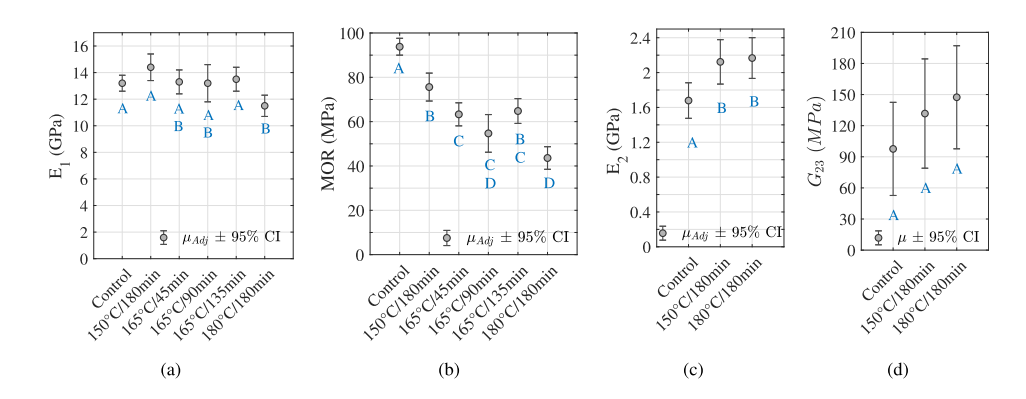


Fig. 10. Effects of thermal modification in three-point bending properties: (a) Modulus of elasticity parallel to the grain (E_1), (b) MOR parallel to the grain, (c) shear free orthogonal modulus of elasticity (E_2), and (d) shear modulus (G_{23}). Groups with the same letter are not significantly different (p-value < 0.05).

with higher temperature and time in TM. Paul et al. [37] conducted a TM process on Scots pine wood-strands prior to the manufacture of OSB and found no significant change in bending stiffness (MOE) values when using pMDI resin. However, strength values significantly decreased with TM, with 35% to 50% lower values than the controls.

Comparable trends to E were observed in the crystallinity index $(C_r I)$ of thermally modified strands (Fig. 6), with a slight increase and a subsequent drop as TM temperature increases, which can explain in part the apparent change in Young's modulus, in addition to the expected degradation of wood constituents through the treatment as seen later (see Fig. 8). Bhuiyan et al. [70] also reported an initial increase in the $C_r I$ under pressurized treatment conditions as these conditions intensify, with a subsequent drop. Esteves and Pereira [24] reported that during TM, cellulose crystallinity is increased due to the partial degradation of amorphous cellulose.

SFE was found to increase with TM temperature (Fig. 7); however, the contact angles obtained at TM temperatures of 150 °C through 180 °C, which were used to compute *SFE*, were found to not be significantly different (Table 2). Based on this finding, there is not enough evidence to state that SFE continues to increase as temperature increases after 150 °C, which is the case of treatments at 165 °C and

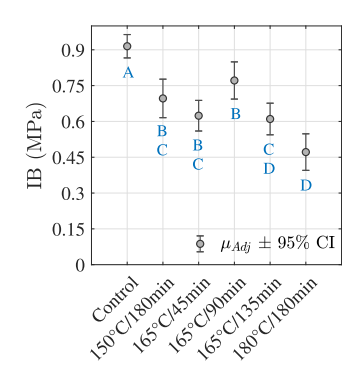
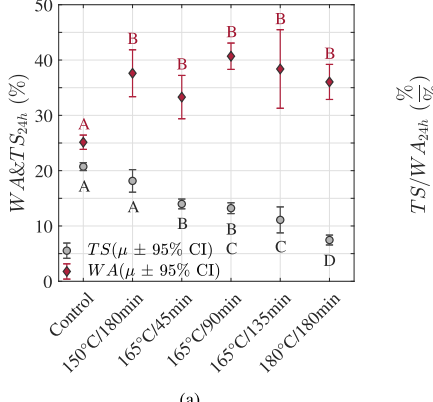


Fig. 11. Effect of thermal modification on IB strength of wood-strand composite panels. Groups with the same letter are not significantly different (p-value < 0.05).

180 °C for 180 min. Yet, it is important to point out the trend in the increase of *SFE*. The same can be said about the polar ratio, γ^p/γ , which increases from 2.5% to approximately 13% as temperature increases; however, the polar ratio is significantly different only between the



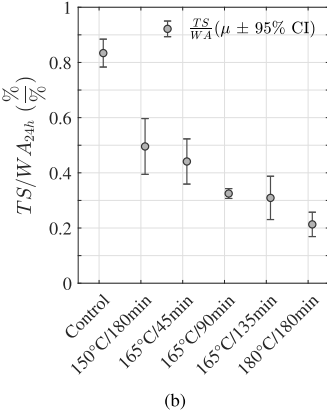
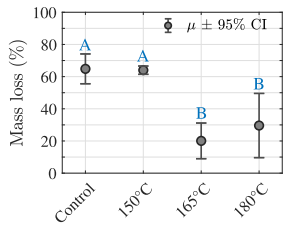
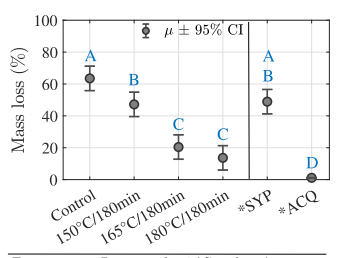


Fig. 12. (a) Water absorption (WA) and thickness swelling (TS) after 24 h submersion of specimens produced from strands modified at different intensities. Groups with the same letter are not significantly different (*p*-value < 0.05); (b) decreasing ratio of TS/WA at 24-h indicates greater dimensional stability of the material with increasing thermal modification intensity.



Exposure to: Brown rot fungi (G. trabeum)
Time: 39 days



Exposure to: Brown rot fungi (G. trabeum)
Time: 55 days
Sample size: 5 samples/group
*Reference values (SYP: Southern yellow pine, ACQ:

Alkaline copper quaternary treatment)

(a) Wood-strands

Sample size: 5 strands/group

(b) Wood-strands composite panels

Fig. 13. Weight loss from fungal decay test in (a) wood-strands, and (b) wood-strand composite panels and untreated and ACQ-treated SYP lumber.

control group and the thermally modified strands. Nevertheless, despite the increase in *SFE*, the wood surface becomes more hydrophobic, as reflected by the increased contact angle with distilled water (Table 2).

Similar to SFE, the K-value obtained from the Shi and Gardner model increases as TM temperature increases (Fig. 7). This result implies a higher penetration and spreading of pMDI resin, and thus better wettability, which can be attributed to the increase in SFE and, expectedly, in porosity within the modified wood strands, as seen in previous studies [49,71,72]. Kutnar et al. [71] also reported an increase in contact angle and SFE as TM intensity increased. Likewise, Croitoru et al. [72] found an increase in SFE and in polar ratio as treatment conditions became more intense; e.g., temperature and dwell time. Changes in SFE partially result from the removal of -OH groups on the surface of wood due to the degradation of hemicelluloses. The chemical composition analysis showed that the changes in composition become more evident as treatment temperature increased (Fig. 8). However, at low treatment intensity (i.e., 150 °C) no visible changes occur. As the temperature increased (with dwell time of 180 min), the most apparent change is in the relative increase of total lignin, mostly with Klason lignin and to a lesser extent acid-soluble lignin. This relative increase in lignin content results from the partial removal of sugars that make up hemicelluloses, as it can be observed from the reduction of total neutral sugars. As expected, the decrease of hemicelluloses is proportional to the TM temperature, with the most intensive treatment exhibiting the largest decrease. Lower hemicelluloses content makes wood more hydrophobic and more resistant to fungal decay [18,28]. It is interesting to note that the reduction of hemicelluloses during the TM process is not as high as in the case of other wood TM processes, such as hot water extraction (HWE) [19]. The removal of hemicelluloses

degradation products in HWE results in part from the extraction of the water after the process, which is not the case of the TM process used in this work. The presence of some moisture in the materials under treatment aids the partial removal of hemicelluloses via hydrolysis, but the use of high pressure in the equipment increases the waterboiling point, which avoids drastic water evaporation and part of the moisture remains in the wood cells, thus avoiding the removal of higher amounts of hemicelluloses degradation products. Altgen et al. [41] also observed this phenomenon and noted that high pressures during treatment prevent the excessive vaporization of hemicelluloses degradation products.

The moisture affinity of the thermally modified strands can be examined by observing the sorption isotherms for strands modified at different temperatures and dwell time in Fig. 9. The isotherms show that the sorption capacity of the thermally modified wood diminishes with increasing TM temperature (Fig. 9(a)), while dwell time does not impart a significant change in the sorption until it reaches 180 min (Fig. 9(b)). An interesting observation arises when examining the absorption curve of wood-strands modified at 165 °C/180 min, which shows a lower sorption capacity than the wood-strands thermally modified at 180 °C/180 min. This is unexpected as it is believed that the higher treatment intensities result in lower sorption capacity. However, this could be influenced by a higher degree of crystallinity found in the group treated at 165 °C/180 min (see Fig. 6) compared to that treated at 180 °C/180 min. It has been noted that an increase in crystallinity results in a lowered accessibility of -OH groups to water molecules [73–75]. Nevertheless, it is difficult to assure a lowered sorption curve at the 165 °C treatment over the 180 °C treatment, since the variability of results reflects that both curves could be similar. When fitting the measured points to the GAB model, the C parameter could not be determined given that there was not enough data in the 5%-15% RH range. However, if we force EMC to be 0% at 0% RH, the values for C that minimize the error in the non-linear fitting become large (i.e., C = 999). This suggests a strong bound of water molecules to the first formed monolayer.

The other parameters for the GAB model are shown in Table 3. For instance, M_m appears to be reduced with TM, decreasing the capacity of the material to retain water molecules within the first layer, which is more tightly bound to the sorbent surface. Likewise, K_{GAB} is also reduced with TM, with the lower value obtained after the 165 °C/180 min TM. This implies that with TM, more sorbed molecules are structured in the multilayer, and behave less like liquid water molecules [76]. The adsorption intake comes from the changes in the chemical composition of the thermally modified wood (Fig. 8) as higher amounts of lignin and lower amounts of hemicelluloses promote hydrophobicity to the modified strands.



Fig. 14. (a) Four-point bending shear failure of a CLSVL beam $(1/h \ge 20)$ made of control strands, (b) premature glue line failure of four-point bending CLSVL beam $(1/h \ge 20)$ made of thermally modified strands, (c) three-point bending shear failure of a CLSVL beam $(1/h \le 5)$ made of control strands, and (d) three-point bending shear failure of a CLSVL beam $(1/h \le 5)$ made of thermally modified strands.

3.2. Mechanical performance of wood-strand composite panels

The modulus of elasticity parallel to the grain direction (E_1) from the static three-point bending results are shown in Fig. 10(a). It is seen that TM causes a slight stiffening of the material at lower thermal modification intensity, with the effect reduced as the intensity increases, which is in agreement with the tendency observed in the tensile Young's modulus of the thermally modified wood-strands (Fig. 5). Again, this stiffening effect may be explained by the increased relative degree of crystallinity of strands as previously discussed. Nevertheless, the MOR decreases as TM intensity increases (Fig. 10(b)), which is also observed for the UTS of the strands (Fig. 5). Similar to the UTS values on wood-strands, the decrease in strength results from the degradation of hemicelluloses and possibly some non-crystalline cellulose during the TM process. However, the positive correlation between density and MOR values (p-value < .0001 from the model utility test) suggests that, to some degree, densification could help to minimize the strength loss of panels produced with thermally modified strands. It is known that TM may help to reduce the springback effect resulting from hot pressing of panels [77] and wood chips, as confirmed by other studies using HWE [78]. The shear free modulus of elasticity along direction 2 (See Fig. 3), E_2 , and shear modulus (G_{23}) results are shown in Figs. 10(c) and 10(d), respectively. As in the case with E_1 , E_2 also exhibits a slight increase as the TM intensity increases. However, there is not enough evidence to suggest there is an increase in G_{23} when TM intensity is increased.

Internal bond (IB) strength results (Fig. 11) show that TM has a slight negative impact on IB values. Lower IB strength is seen as TM intensity increases. In addition to increased material brittleness at higher thermal modification temperatures, MC in the wood-strands could affect these results since pMDI resin used in the manufacture of the panels uses water for the curing reaction. Guangbo and Yan [79] reported that there is a significant effect on cure kinetics of isocyanate due to moisture in wood. Although -OH groups in the wood may react with the isocyanate to form chemical bonds between the adhesive and wood, reactions of pMDI with water to form polyurea were dominant when moisture was present. Thus, the addition of water to the woodstrands could help to improve the bond between strands. This practice could be easily implemented in the manufacturing process as moisture can be added before the hot-pressing process. However, it has been observed that MC over 12% no longer has a significant effect on the cure kinetics [79].

Results of the water absorption (WA) and thickness swelling (TS) of the panels after the 24 h submersion are shown in Fig. 12(a). Within

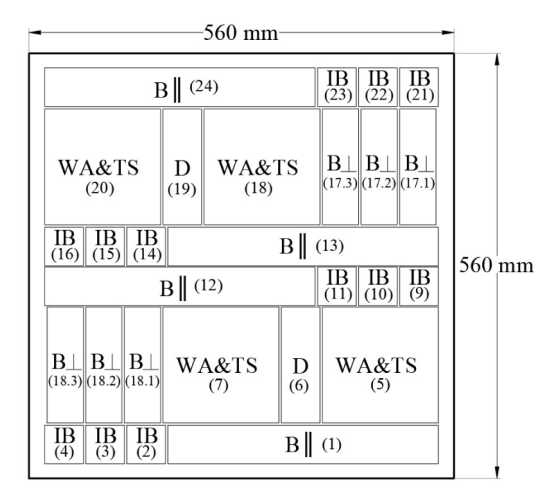


Fig. 15. Specimen sampling from fabricated panels from 889×889 mm hydraulic press. B|| for bending parallel to the strands' main orientation, with dimensions 50.8 \times 355.6 mm; B⊥ for bending perpendicular to the strands' main orientation, with dimensions 25.4×152.4 mm; IB for internal bond (and also used for vertical density profile (VDP)), with dimensions 50.8×50.8 mm; WA&TS for water absorption and thickness swell with dimensions 152.4×152.4 mm; and D for decay, with dimensions 50.8×152.4 mm.

the range tested in this study, WA increased as the intensity of TM increased. This change may be due to an increase in porosity of the strands after undergoing TM. Conversely, TS values are significantly reduced as TM intensifies; therefore, wood strands and the manufactured composite materials may have greater dimensional stability. To better understand the trend of the panels' behavior in presence of water, the TS/WA ratio is presented in Fig. 12(b). The decreasing TS/WA ratio with increased TM intensity suggests that the water in thermally modified wood does not necessarily account for physical changes in the wood cell; rather, it is free water within the voids of wood.

As a way of comparison to the control and thermally modified wood-strand panels, some benchmark values from different types of commercially available products are presented in Table 4. Weight and Yadama [43] developed a laminated strand veneer (LSV) with wood species and strand geometry similar to that presented in this work, although phenol–formaldehyde (PF) resin was used instead of pMDI, and the thickness of the laminates were 3.2 mm. The control group performed similar to the LSV from the referred work, but higher bending MOE and IB strength values were reported. Commercially

Table 4Comparison of properties between commercially available products and panels produced with thermally modified strands.

		Static bendir	ng						
		Modulus of elasticity		Modulus of rupture		IB	TS_{24h}	WA_{24h}	
Reference	Species	Product	II	Τ	II			- 2411	2411
			GPa		MPa		MPa	%	%
This work	ESLP	Control panels	13.2	1.7	93.8	-	0.91	20.7	25.1
This work	ESLP	thermally modified panels	11.5-14.4	2.2	43.6-75.6	_	0.47 - 0.77	7.5-18.2	36.0-40.7
[43]	Ponderosa pine	LSV	10.4	1.1	91.1	14.3	0.61		
[80]	Southern pine	LVL	8.8-13.0	_	47.8-66.5	_	_	_	_
[81]	Ponderosa pine	SD glulam	9.1-9.4	_	29.6-31.4	_	_	-	-
[82,83]	Aspen poplar	LSL	11.6	1.3	61.7	8.9	_	_	_
[84]	Southern pine	OSB	4.9-5.3	2.2 - 2.6	28.1-30.7	14.4-21.1	0.32 - 0.43	16.3	29.3
ICC	_	OSB ^a	7	3	$25-30^{b}$	14–18 ^b	_	-	-
[85]	Ponderosa pine	SD No. 1	6.4	_	30.7	_	_	-	-
[85]	Lodgepole pine	SD No. 1	10.2	-	45.3	-	-	-	-

^aWeyerhaeuser DiamondTM Floor Panels - ICC-ES ESR-4133.

Table 5
Out-of-plane bending results.

			Apparent i	_ τ ₁₃		
Loading condition	Beam type	l/h	Measured	Predicted	Error	13
			GPa		%	MPa
4-point-bending	Control	20.8	11.9	11.8	-0.8	1.0
4-point-bending	TM^b	24.2	12.2	12.6	3.3	0.2^{a}
	Control	4.4	1.4	1.2	-15.4	1.3
3-point-bending	Control	4.4	1.2	1.2	4.2	1.8
	TM ^b	5.0	1.9	1.9	-2.2	1.1

^aPremature failure at PUR glue line

available Southern pine laminated veneer lumber (LVL) used for structural purposes has lower MOE than the control and thermally modified wood strand panels and similar MOR values than the panels with the most intense TM (180 °C/180 min). Glue laminated timber made from small-diameter ponderosa pine, similar to the wood species used in this work, has overall lower MOE and MOR values. Laminated strand lumber, frequently used for structural elements in trusses, headers, wall studs, roof beams, and rafters has lower MOE values and about 35% higher MOR values than the manufactured panels with the most intense TM (See Table 4). Two different oriented strand board (OSB) products were also used for comparison (See Table 4). The first one made of Southern pine had lower MOE, MOR, and IB strength than the control and thermally modified panels, with WA and TS values similar to the control group after 24 h submersion, and significantly higher TS than the thermally modified composite from this work. The other OSB used as a reference is a commercially available premium product, with overall lower mechanical performance. Lastly, the MOE and MOR values from two No. 1 visually graded small-diameter ponderosa and lodgepole pine dimensional lumber products are presented, reflecting a lower performance than the thermally modified panels reported herein.

3.3. Decay resistance

Results from the accelerated decay tests of both strands and panels are shown in Fig. 13. It is seen that, as the TM temperature increases, both materials (i.e., strands and panels in Figs. 13(a) and 13(b), respectively) become more resistant to the brown rot fungus Gloeophyllum trabeum. In the case of the panels, two additional groups were also examined for comparison: (a) samples of Southern yellow pine (SYP) solid wood specimens and (b) ACQ-treated SYP specimens. The ACQ-treated specimens were more resistant to G. trabeum fungi than panels manufactured from thermally modified wood, as tested. However, it is evident that thermal modification significantly improves

Table 6Total number of specimens used for testing.

	No. of panels	В∥	В⊥	IB	VDP	WA&TS	
Cotrol	5	20	12	60	60	20	
150 °C/180 min	2	8	8	24	24	8	
165 °C/45 min	3	12	-	36	36	12	
165 °C/90 min	2	8	-	24	24	8	
165 °C/135 min	3	12	-	36	36	12	
165 °C/180 min	-	-	-	-	-	-	
180 °C/180 min	3	12	12	36	36	12	
TOTAL	18	72	32	216	216	72	

the fungal decay resistance of panels produced with thermally modified strands, suggesting that more hydrophobic strands improved long-term durability of panels. Increased decay resistance of materials undergoing TM results from the reduction of hemicelluloses in wood fibers since it is known that modified wood reduces the amount of available water needed for fungi to colonize wood cells [86].

3.4. Out-of-plane flexural performance of CLSVL

In order to model the out-of-plane bending behavior of CLSVL, material properties (E_1 and E_2) from the 1220×2440 mm panels used for the fabrication of the 15-ply CLSVL beams were determined from bending specimens, as described in Section 2.4. The values obtained in this case were $E_1 \approx 7$ GPa and $E_2 \approx 3$ GPa, which are considerably different than the values shown in Fig. 10 (panels made with the 889 × 889 mm hydraulic press). For instance, the strand's orientation was likely causing the difference, as E_1/E_2 ratio was only 2.33, meaning that the strand's grain orientation was above the $\pm 30^\circ$ target from axis 1 (Fig. 3). Nevertheless, if the strand's orientation issue is resolved, then mechanical properties from the 1220×2440 mm panels would be expected to be closer to the previously reported values in Section 3.2.

^bEstimated from allowable stress design (ASD) values assuming these correspond to the 5th percentile of normally distributed data with coefficient of variation between 15%–25% and a reduction factor of 2.1 as established by ASTM D1990.

^bPanel made of 165 °C/180 min thermally modified strands only.

Table 7
ANOVA analysis.

P-value								
	ANCOVA							
	Separate lines model $y = (\alpha + \alpha_i) + (\beta + \beta_i)x + \epsilon$		Parallel lines model $y = (\alpha + \alpha_i) + \beta x + \epsilon$		Model assumpt			
					Normality		Homoscedasticity	
Response\Factor	A	В	$A \times B$	A	В	Shapiro-Wilk	Anderson–Darling	Levene
Youngs modulus, E (Fig. 5(a))	0.118	<.0001	0.172	0.011	<.0001	0.229	>0.250	0.803
Youngs modulus, E (Fig. 5(c))	0.840	<.0001	0.802	0.155	<.0001	0.155	>0.250	0.058
Ultimate tensile strength, UTS (Fig. 5(b))	0.179	<.0001	0.128	<.0001	<.0001	0.083	0.034	0.740
Ultimate tensile strength, UTS (Fig. 5(d))	0.204	0.003	0.255	<.0001	<.0001	0.885	>0.250	0.484
Modulus of elasticity, MOE_1 (Fig. 10(a), left)	0.001	<.001	0.094	0.002	0.001	0.034	0.124	0.559
Modulus of rupture, MOR_1 (Fig. 10(b), left)	0.001	0.097	0.409	<.001	0.094	0.053	0.042	0.787
Modulus of elasticity, MOE_1 (Fig. 10(a), right)	0.047	<.0001	0.065	0.002	<.0001	0.967	>0.250	0.318
Modulus of rupture, MOR_1 (Fig. 10(b), right)	0.667	<.0001	0.371	<.0001	<.0001	0.224	0.192	0.790
Modulus of elasticity, MOE_2 (Fig. 10(c))	0.235	<.0001	0.133	0.007	<.0001	0.564	>0.250	0.203
Shear modulus, G_{23} (Fig. 10(d))	0.575	0.186	0.536	0.254	0.152	0.080	0.075	0.416
Internal bond strength, IB (Fig. 11)	0.138	<.0001	0.017	<.0001	<.0001	0.185	>0.250	0.108
	One-way ANOVA							
	$y_{ij} = \alpha_j +$	ϵ_{ij}				-		
Degree of crystallinity, CrI (Fig. 6)	<.0001	-	-	-	-	0.539	>0.250	0.591
Thickness swell, TS (Fig. 12(a))	<.0001	_	_	_	_	_	_	_
Water absorption, WA (Fig. 12(a))	<.0001	_	_	_	_	_	_	_
Wood-strands decay resistance (Fig. 13(a))	<.0001	-	_	-	_	0.111	0.0987	0.370
Panels decay resistance (Fig. 13(b))	<.0001	_	_	_	_	0.278	>0.250	0.397

A: Treatment; B: Density/Bolded values are significant ($\alpha = 0.05$)

On the other hand, since G_{23} and G_{13} were found to be similar from previous testing (Fig. 10), it is assumed that this material's property is not affected by the forming process. Consequently, the following material properties were implemented in Eqs. (7)–(8) to predict the out-of-plane bending behavior of CLSVL: $E_1 = 7$ GPa and $E_2 = 3$ GPa for the control and thermally modified panels (165 °C/180 min), $G_{13} = G_{23} = 0.1$ GPa for the control panels, and $G_{13} = G_{23} = 0.13$ GPa for the thermally modified panels (165 °C/180 min).

Table 5 shows the results from the out-of-plane bending in the 15-ply CLSVL specimens. It can be observed than the Shear Analogy Method accurately predicts the stiffness and deflections of CLSVL under different loading configurations and different span-to-depth ratios, 1/h. This was verified for both scenarios: CLSVL made of control strands, and CLSVL made of thermally modified strands. It is expected that with more accurately estimated panel material properties (E_1 , E_2 , G_{12} , and G_{23}) the bending behavior prediction of CLSVL will be even more accurate. This could be more easily achieved in the industry through the use of controlled manufacturing protocols.

The failing mechanism for each beam was visually assessed, finding that in all cases a shear failure occurred (Fig. 14). The loading caused the wood fibers near the core laminates (transverse or orthogonal plies) to fail and extend mostly horizontally from the point of loading towards the support. The maximum load at which the beams failed was measured and used to estimate the shear limit state are shown in the last column of Table 5. For instance, the CLSVL beam made from thermally modified strands under four-point bending had a premature failure at the PUR glue line. The manual application of the PUR resin with a roller could have caused a non-uniform application of the adhesive, leaving some sections of the bond surface with less resin. Moreover, since this premature failure did not occur in the other CLSVL beam made of thermally modified strands, it is thought that the TM is not affecting the bonding performance with PUR, although further research on this matter is necessary. Nevertheless, without consideration of the specimen with premature failure at the glue line, no major difference is observed in the estimated maximum shear stress values between the control and the thermally modified composite panels. Yet, this cannot be conclusive since the sample size is small and statistical analysis could not be performed; thus, further testing would be required. Mass timber products such as CLT often fail due to rolling shear, which is minimized, if not eliminated, in wood strand-based mass timber

products as reported elsewhere [82,87,88]. The CLSVL beams in this study did not experience a rolling shear type failure either. Despite this, the shear capacity of the CLSVL beams appear to be in the range of values of traditional CLT, with strength capacity ranging between 1 to 3 MPa [88,89]. However, a larger sample size is necessary to accurately estimate the shear strength capacity.

The findings shown herein establish a proof-of-concept for the use of thermally modified wood-strand composites to be used as engineering products. The CLSVL beams studied in this work are likely suitable for a wide range of applications as structural elements in high moisture environments. Furthermore, the thermally modified wood-strand panels could also be used to fabricate tailored composite products for different applications. For instance, the laminates could all be oriented and bonded parallel to the direction of the grain to build mass timber panels (as opposed to traditional CLT, which is manufactured from perpendicular laminations), or in another scenario, the orientation of the wood strands, while forming the panels, could be set to $\sim 45^{\circ}$ from axis 1 (see Fig. 3) in order to use the panel as a web in a wood joist so that shear performance is maximized. Also, other optimal layouts could be used to ensure that specific performance requirements are met. Thus, with the continued growth of mass timber construction, this work provides further performance improvements while making use of underutilized small diameter timber.

4. Conclusions

The present work focuses on the development of durable wood strand composites from thermally modified Engelmann spruce and lodgepole pine strands. Thermal modification intensity, in terms of dwell time and temperature, had no significant effect on tensile modulus of elasticity. However, temperature played a significant role on tensile strength, with higher temperatures leading to lower strength. The water wettability and hygroscopicity of the thermally modified wood-strands was reduced, while surface free energy was found to increase, possibly improving the wetting of pMDI resin used for the manufacture of wood-strand composites. Moreover, a slight increase in the degree of crystallinity was observed as TM temperature increased, with an indication of a subsequent drop as treatment conditions become more intense. This change in relative degree of crystallinity may be the reason why the tensile modulus of elasticity was unaffected or slightly

increased, depending on treatment intensity. The increase in degree of crystallinity may also impart moisture resistance, since its structure may result in reduced accessibility of water molecules to -OH groups. There was not a significant effect on bending modulus of elasticity of manufactured panels made of thermally modified wood-strands, although a slight increase may exist. However, modulus of rupture in the panels was reduced by TM, primarily by treatment temperature and, to a lesser extent, dwell time. The internal bond strength was reduced with TM intensity. Likewise, TM significantly reduced the thickness swell of the composite panels. An indirect measurement of dimensional stability, TS/WA ratio, was found to significantly decrease with increasing TM intensity, indicating the resulting product to be more dimensionally stable in moisture rich environments. The decrease of this ratio suggests that the bound water capacity is reduced with TM. Lastly, TM improved decay resistance when the wood-strands and wood-strand composite panels were exposed to brown rot fungi G. trabeum. These factors may be attributed to the removal of hemicelluloses which serve as an alimentary source to fungi. Despite the strength reduction with TM, the mechanical performance of the thermally modified woodstrand composite panels is similar to or better than other wood-based materials commonly used in structural applications. Also, TM could reduce the counterproductive springback effect after hot-pressing, giving opportunity to densification of panels and hence improved mechanical properties. The shear analogy method was found to be an appropriate way to model the out-of-plane bending behavior of CLSVL, even for the case of thermally modified wood-strands. The model accurately predicted the bending stiffness of the tested beams under different span-to-depth ratios and loading conditions (three-point bending and four-point bending). In general, the implementation of the discussed TM process likely increases the prospective service life of the material by reducing the moisture intake and improving decay resistance and dimensional stability.

CRediT authorship contribution statement

Ruben Jerves: Methodology, Software, Formal analysis, Investigation, Data curation, Writing – original draft, Visualization. Vikram Yadama: Conceptualization, Supervision, Writing – review & editing, Project administration, Resources, Funding acquisition. Matthew Aro: Conceptualization, Investigation, Writing – review & editing, Funding acquisition. Manuel Raul Pelaez-Samaniego: Investigation, Writing – review & editing.

Declaration of competing interest

The authors declare that they have no known competing financial interests or personal relationships that could have appeared to influence the work reported in this paper.

Data availability

Data will be made available on request.

Acknowledgments

This material is based upon work supported by the National Science Foundation, United States under Grant No. 1827434. Thank you to Professor Armando McDonald and Dr. Abdulbaset Alayat (Department of Forest, Rangeland and Fire Sciences, University of Idaho) for their assistance in conducting the chemical composition analysis. We also acknowledge the Forest and Wildlife Research Center, Department of Sustainable Bio-products at Mississippi State University, for assistance in performing the decay tests.

References

- American National Standards Institutes ANSI/APA, ANSI/APA prg 320-2018:
 Standard for performance-rated cross-laminated timber, 320, 2018, pp. 1–33.
- [2] J.L. Shi, S.Y. Zhang, B. Riedl, Effect of juvenile wood on strength properties and dimensional stability of black spruce medium-density fiberboard panels, 59, (1) 2005, pp. 1–9, http://dx.doi.org/10.1515/HF.2005.001.
- [3] R.J. Ross, F.P.L. USDA Forest Service, Wood Handbook: Wood as an Engineering Material, Technical Report, 2010, http://dx.doi.org/10.2737/FPL-GTR-190, https://www.fs.usda.gov/treesearch/pubs/37440.
- [4] S.L. Levan-Green, J. Livingston, Exploring the uses for small-diameter trees, For. Prod. J. 51 (9) (2001) 10–21.
- [5] M. Fredriksson, P. Bomark, O. Broman, A. Grönlund, Using small diameter logs for cross-laminated timber production, BioResources 10 (1) (2015) 1477–1486, http://dx.doi.org/10.15376/biores.10.1.1477-1486.
- [6] H. Heräjärvi, A. Jouhiaho, V. Tammiruusu, E. Verkasalo, Small-diameter scots pine and birch timber as raw materials for engineered wood products, Int. J. For. Eng. 15 (2) (2004) 23–34, http://dx.doi.org/10.1080/14942119.2004.10702494.
- [7] O. Geiger, Small-diameter wood: An underused building material | Natural building blog, 2015.
- [8] G. Wu, E. Zhu, H. Ren, M. Gong, Use of small-diameter round timber as structural members in light frame construction, in: ST107-1 Building Tomorrow's Society Bâţir la Société de Demain, 2018.
- [9] D. Paun, G. Jackson, Potential for Expanding Small Diameter Timber Market: Assessing Use of Wood Posts in Highway Applications, Technical Report, U.S. Department of Agriculture, Forest Service, Forest Products Laboratory, 2000, http://dx.doi.org/10.2737/FPL-GTR-120.
- [10] J. Livingston, Small-Diameter Success Stories, Technical report, U.S. Department of Agriculture, Forest Service, Forest Products Laboratory, Madison, WI, 2004, https://www.fpl.fs.fed.us/documnts/fpmu/sd{_}success{_}stories.pdf.
- [11] H. Sivonen, S.L. Maunu, F. Sundholm, S. Jämsä, P. Viitaniemi, Magnetic resonance studies of thermally modified wood, Holzforschung 56 (6) (2002) 648–654, http://dx.doi.org/10.1515/HF.2002.098.
- [12] M. Hakkou, M. Pétrissans, A. Zoulalian, P. Gérardin, Investigation of wood wettability changes during heat treatment on the basis of chemical analysis, Polym. Degrad. Stab. 89 (1) (2005) 1–5, http://dx.doi.org/10.1016/J. POLYMDEGRADSTAB.2004.10.017.
- [13] D. Kocaefe, S. Poncsak, Y. Boluk, Effect of thermal treatment on the chemical composition and mechanical properties of birch and aspen, BioResources (2008) 517-537.
- [14] V. Repellin, R. Guyonnet, Evaluation of heat-treated wood swelling by differential scanning calorimetry in relation to chemical composition, Holzforschung 59 (1) (2005) 28–34, http://dx.doi.org/10.1515/HF.2005.005.
- [15] H. Spelter, D. McKeever, D. Toth, Profile 2009: softwood Sawmills in the United States and Canada, Technical Report, U.S. Department of Agriculture, Forest Service, Forest Products Laboratory, Madison, WI, 2009, http://dx.doi.org/10. 2737/FPL-RP-659.
- [16] B. Tjeerdsma, M. Stevens, H. Militz, J. Van Acker, Effect of process conditions on moisture content and decay resistance of hydro-thermally treated wood. | Semantic scholar, Holzforsch. Verwert. (1971) 94–99.
- [17] J.J. Weiland, R. Guyonnet, Study of chemical modifications and fungi degradation of thermally modified wood using DRIFT spectroscopy, Holz Roh Werkst. 61 (3) (2003) 216–220, http://dx.doi.org/10.1007/s00107-003-0364-y.
- [18] C.A.S. Hill, Wood Modification: Chemical, Thermal and Other Processes, 2006, pp. 1–239, http://dx.doi.org/10.1002/0470021748.
- [19] M.R. Pelaez-Samaniego, V. Yadama, E. Lowell, R. Espinoza-Herrera, A review of wood thermal pretreatments to improve wood composite properties, Wood Sci. Technol. 47 (6) (2013) 1285–1319, http://dx.doi.org/10.1007/s00226-013-0574-3.
- [20] M.J. Boonstra, J. Van Acker, B.F. Tjeerdsma, E.V. Kegel, Strength properties of thermally modified softwoods and its relation to polymeric structural wood constituents, Ann. For. Sci. 64 (7) (2007) 679–690, http://dx.doi.org/10.1051/ forest:2007048.
- [21] Y. Zheng, Z. Pan, R. Zhang, B.M. Jenkins, S. Blunk, Properties of medium-density particleboard from saline Athel wood, Ind. Crop. Prod. 23 (3) (2006) 318–326, http://dx.doi.org/10.1016/j.indcrop.2005.09.003.
- [22] M.N. Anglès, F. Ferrando, X. Farriol, J. Salvadó, Suitability of steam exploded residual softwood for the production of binderless panels. Effect of the pretreatment severity and lignin addition, Biomass Bioenergy 21 (3) (2001) 211–224, http://dx.doi.org/10.1016/S0961-9534(01)00031-9.
- [23] W.E. Hsu, W. Schwald, J. Schwald, J.A. Shields, Chemical and physical changes required for producing dimensionally stable wood-based composites, Wood Sci. Technol. 22 (3) (1988) 281–289, http://dx.doi.org/10.1007/BF00386023.
- [24] B.M. Esteves, H.M. Pereira, Wood modification by heat treatment: A review, Bioresources 4 (1965) (2009) 370–404, http://dx.doi.org/10.15376/biores.4.1. 370-404.
- [25] K. Candelier, M.F. Thevenon, A. Petrissans, S. Dumarcay, P. Gerardin, M. Petrissans, Control of wood thermal treatment and its effects on decay resistance: A review, Ann. For. Sci. 73 (3) (2016) 571–583, http://dx.doi.org/10.1007/s13595-016-0541-x.

- [26] F. Shafizadeh, P.P.S. Chin, Thermal deterioration of wood, in: Wood Technology: Chemical Aspects, 1977, pp. 57–81, http://dx.doi.org/10.1021/bk-1977-0043. ch005
- [27] W.E. Hillis, High temperature and chemical effects on wood stability part 1: General considerations, Wood Sci. Technol. 18 (4) (1984) 281–293, http://dx.doi.org/10.1007/BF00353364.
- [28] O. Hosseinaei, S. Wang, A.A. Enayati, T.G. Rials, Effects of hemicellulose extraction on properties of wood flour and wood-plastic composites, Composites A 43 (4) (2012) 686–694, http://dx.doi.org/10.1016/j.compositesa.2012.01.007.
- [29] P. Mitchell, Irreversible property changes of small loblolly pine specimens heated in air, nitrogen, or oxygen, Wood Fiber Sci. 20 (3) (1988) 320–335.
- [30] V. Caprai, F. Gauvin, K. Schollbach, H.J.H. Brouwers, Influence of the spruce strands hygroscopic behaviour on the performances of wood-cement composites, Constr. Build. Mater. 166 (2018) 522–530, http://dx.doi.org/10.1016/j. conbuildmat 2018 01 162
- [31] T. Ding, L. Gu, L. Xiang, Influence of steam pressure on chemical changes of heat-treated mongolian pine wood, BioResources 6 (2) (2011) 1880–1889, http://dx.doi.org/10.15376/BIORES.6.2.1880-1889.
- [32] M. Hakkou, M. Pétrissans, P. Gérardin, A. Zoulalian, Investigations of the reasons for fungal durability of heat-treated beech wood, Polym. Degrad. Stab. 91 (2) (2006) 393–397, http://dx.doi.org/10.1016/j.polymdegradstab.2005.04.042.
- [33] O. Unsal, S.N. Kartal, Z. Candan, R.A. Arango, C.A. Clausen, F. Green, Decay and termite resistance, water absorption and swelling of thermally compressed wood panels, Int. Biodeterioration Biodegrad. 63 (5) (2009) 548–552, http: //dx.doi.org/10.1016/j.ibiod.2009.02.001.
- [34] Y. Kubojima, T. Okano, M. Ohta, Bending strength and toughness of heat-treated wood, J. Wood Sci. 46 (1) (2000) 8–15, http://dx.doi.org/10.1007/BF00779547/ MFTRICS
- [35] S. Ates, M. Hakan Akyildiz, H. Ozdemir, Effects of heat-treatment on calabrian pine wood, BioResources 4 (3) (2009) 1032–1043.
- [36] J.L. Shi, D. Kocaefe, J. Zhang, Mechanical behaviour of Québec wood species heat-treated using ThermoWood process, Holz Roh Werkst. 65 (4) (2007) 255–259, http://dx.doi.org/10.1007/S00107-007-0173-9.
- [37] W. Paul, M. Ohlmeyer, H. Leithoff, M.J. Boonstra, A. Pizzi, Optimising the properties of OSB by a one-step heat pre-treatment process, Holz Roh Werkst. 64 (3) (2006) 227–234, http://dx.doi.org/10.1007/s00107-005-0073-9.
- [38] M.J. Boonstra, A. Pizzi, M. Ohlmeyer, W. Paul, The effects of a two stage heat treatment process on the properties of particleboard, Holz Roh Werkst. 64 (2) (2006) 157–164, http://dx.doi.org/10.1007/s00107-005-0055-y.
- [39] W. Paul, M. Ohlmeyer, H. Leithoff, Thermal modification of OSB-strands by a one-step heat pre-treatment — influence of temperature on weight loss, hygroscopicity and improved fungal resistance, Holz Roh Werkst. 65 (1) (2007) 57-63, http://dx.doi.org/10.1007/s00107-006-0146-4.
- [40] J.J. Paredes, R. Jara, S.M. Shaler, A. Van Heiningen, Influence of hot water extraction on the physical and mechanical behavior of OSB, For. Prod. J. 58 (12) (2008) 56-62.
- [41] M. Altgen, W. Willems, H. Militz, Wood degradation affected by process conditions during thermal modification of European beech in a high-pressure reactor system, Eur. J. Wood Wood Prod. 74 (5) (2016) 653–662, http://dx.doi. org/10.1007/s00107-016-1045-y.
- [42] C. Hill, M. Altgen, L. Rautkari, Thermal modification of wood—A review: Chemical changes and hygroscopicity, J. Mater. Sci. 56 (11) (2021) 6581–6614, http://dx.doi.org/10.1007/s10853-020-05722-z.
- [43] S.W. Weight, V. Yadama, Manufacture of laminated strand veneer (LSV) composite. Part 1: Optimization and characterization of thin strand veneers, Holzforschung 62 (6) (2008) 718–724, http://dx.doi.org/10.1515/HF.2008.126.
- [44] S.W. Weight, V. Yadama, Manufacture of laminated strand veneer (LSV) composite. Part 2: Elastic and strength properties of laminate of thin strand veneers, Holzforschung 62 (6) (2008) 725–730, http://dx.doi.org/10.1515/HF.2008.127.
- [45] N. Kohan, B.K. Via, S. Taylor, A comparison of geometry effect on tensile testing of wood strands, For. Prod. J. 62 (3) (2013) 167–170, http://dx.doi.org/10. 13073/0015-7473-62.3.167.
- [46] G.Y. Jeong, D.P. Hindman, D. Finkenbinder, J.N. Lee, Z.Y. Lin, Effect of loading rate and thickness on the tensile properties of wood strands, For. Prod. J. 58 (10) (2008) 33–37.
- [47] M. De Meijer, S. Haemers, W. Cobben, H. Militz, Surface energy determinations of wood: Comparison of methods and wood species, Langmuir 16 (24) (2000) 9352–9359, http://dx.doi.org/10.1021/la001080n.
- [48] S. Shi, D. Gardner, Dynamic adhesive wettability of wood, Wood Fiber Sci. 33 (1) (2001) 58-68.
- [49] J. Follrich, U. Müller, W. Gindl, Effects of thermal modification on the adhesion between spruce wood (*Picea abies* Karst.) and a thermoplastic polymer, Holz Roh Werkst. 64 (5) (2006) 373–376. http://dx.doi.org/10.1007/s00107-006-0107-y.
- [50] X. Wang, F. Wang, Z. Yu, Y. Zhang, C. Qi, L. Du, Surface free energy and dynamic wettability of wood simultaneously treated with acidic dye and flame retardant, J. Wood Sci. 63 (3) (2017) 271–280, http://dx.doi.org/10.1007/s10086-017-1621-8.
- [51] A.C. Ziglio, M.R. Sardela, D. Gonçalves, Wettability, surface free energy and cellulose crystallinity for pine wood (pinus sp.) modified with chili pepper extracts as natural preservatives, Cellulose 25 (10) (2018) 6151–6160, http: //dx.doi.org/10.1007/s10570-018-2007-9.

- [52] F.M. Fowkes, Attractive forces at interfaces, Ind. Eng. Chem. (1964) http://dx. doi.org/10.1021/ie50660a008.
- [53] F.M. Fowkes, Calculation of work of adhesion by pair potential summation, J. Colloid Interface Sci. (1968) http://dx.doi.org/10.1016/0021-9797(68)90082-9.
- [54] F.M. Fowkes, Donor-acceptor interactions at interfaces, J. Adhes. (1972) http://dx.doi.org/10.1080/00218467208072219.
- [55] T. Young, An essay on cohesion of fluids, Philos. Trans. R. Soc. Lond. 95 (1805) 65–87.
- [56] X. Huang, D. Kocaefe, Y. Boluk, Y. Kocaefe, A. Pichette, Effect of surface preparation on the wettability of heat-treated jack pine wood surface by different liquids, Eur. J. Wood Wood Prod. 70 (5) (2012) 711–717, http://dx.doi.org/10. 1007/s00107-012-0605-z.
- [57] Z. Qin, Q. Gao, S. Zhang, J. Li, Surface free energy and dynamic wettability of differently machined poplar woods, BioResources 9 (2) (2014) 3088–3103, http://dx.doi.org/10.15376/biores.9.2.3088-3103.
- [58] Z.-m. Liu, F.-h. Wang, X.-m. Wang, Surface structure and dynamic adhesive, Wood Fiber Sci. J. Soc. Wood Sci. Technol. 36 (2) (2004) 239–249.
- [59] H.P. Gavin, The Levenburg-Marqurdt algorithm for nonlinear least squares curvefitting problems, 2019, pp. 1–19, http://people.duke.edu/{~}hpgavin/ce281/lm. pdf.
- [60] J. Blahovec, S. Yanniotis, Gab generalized equation for sorption phenomena, Food Bioprocess Technol. 1 (1) (2008) 82–90, http://dx.doi.org/10.1007/s11947-007-0012-3.
- [61] I.D. Hartley, Application of the Guggenheim–Anderson–deBoer sorption isotherm model to Klinki pine (*Araucaria klinkii* Lauterb.), Holzforschung (2000) http: //dx.doi.org/10.1515/HF.2000.111.
- [62] I.D. Hartley, S. Wang, Y. Zhang, Water vapor sorption isotherm modeling of commercial oriented strand panel based on species groups and resin type, Build. Environ. 42 (10) (2007) 3655–3659, http://dx.doi.org/10.1016/j.buildenv.2006. 10.002.
- [63] A. Derkowski, R. Mirski, J. Majka, Determination of sorption isotherms of scots pine (pinus sylvestris l.) wood strands loaded with Melamine-Urea-Phenol-Formaldehyde (MUPF) resin, Wood Res. 60 (2) (2015) 201–210.
- [64] L. Segal, J.J. Creely, A.E. Martin, C.M. Conrad, An empirical method for estimating the degree of crystallinity of native cellulose using the X-Ray diffractometer, Text. Res. J. 29 (10) (1959) 786–794, http://dx.doi.org/10.1177/ 004051755902901003.
- [65] E. Karacabeyli, D. Brad, Hand Book Cross Laminated Timber, 2013, p. 572.
- [66] J. Zhou, Y.H. Chui, M. Gong, L. Hu, Elastic properties of full-size mass timber panels: Characterization using modal testing and comparison with model predictions, Composites B 112 (2017) 203–212, http://dx.doi.org/10.1016/j. compositesb.2016.12.027.
- [67] A. Kassimali, J.N. Craddock, M. Matinrad, Bending and transverse shear stresses in fiber-composite beams by the transformed-section method, Compos. Struct. 5 (1) (1986) 33–49. http://dx.doi.org/10.1016/0263-8223(86)90011-5.
- [68] F.W. Calonego, E.T.D. Severo, A.W. Ballarin, Physical and mechanical properties of thermally modified wood from *E. grandis*, Eur. J. Wood Wood Prod. 70 (4) (2012) 453–460, http://dx.doi.org/10.1007/s00107-011-0568-5.
- [69] D. Sandberg, A. Kutnar, Thermally modified timber: Recent developments in Europe and North America, Wood Fiber Sci. 48 (2015) 28–39.
- [70] M.T.R. Bhuiyan, N. Hirai, N. Sobue, Changes of crystallinity in wood cellulose by heat treatment under dried and moist conditions, J. Wood Sci. 46 (6) (2000) 431–436, http://dx.doi.org/10.1007/BF00765800.
- [71] A. Kutnar, B. Kričej, M. Pavlič, M. Petrič, Influence of treatment temperature on wettability of Norway spruce thermally modified in vacuum, J. Adhes. Sci. Technol. 27 (9) (2013) 963–972, http://dx.doi.org/10.1080/01694243.2012. 727168
- [72] C. Croitoru, C. Spirchez, A. Lunguleasa, D. Cristea, I.C. Roata, M.A. Pop, T. Bedo, E.M. Stanciu, A. Pascu, Surface properties of thermally treated composite wood panels, Appl. Surf. Sci. 438 (2018) 114–126, http://dx.doi.org/10.1016/j.apsusc. 2017.08.193.
- [73] H. Wikberg, S.L. Maunu, Characterisation of thermally modified hard- and softwoods by13C CPMAS NMR, Carbohydr. Polymers (2004) http://dx.doi.org/ 10.1016/j.carbpol.2004.08.008.
- [74] M.T.R. Bhuiyan, N. Hirai, Study of crystalline behavior of heat-treated wood cellulose during treatments in water, J. Wood Sci. 51 (1) (2005) 42–47, http: //dx.doi.org/10.1007/s10086-003-0615-x.
- [75] M.J. Boonstra, B. Tjeerdsma, Chemical analysis of heat treated softwoods, Holz Roh Werkst. 64 (3) (2006) 204–211, http://dx.doi.org/10.1007/s00107-005-0078 4
- [76] E.J. Quirijns, A.J.B. Van Boxtel, W.K.P. Van Loon, G. Van Straten, Sorption isotherms, GAB parameters and isosteric heat of sorption, J. Sci. Food Agric. 85 (11) (2005) 1805–1814, http://dx.doi.org/10.1002/JSFA.2140.
- [77] K. Laine, K. Segerholm, M. Wålinder, L. Rautkari, M. Hughes, Wood densification and thermal modification: Hardness, set-recovery and micromorphology, Wood Sci. Technol. 50 (5) (2016) 883–894, http://dx.doi.org/10.1007/s00226-016-0835-z.
- [78] M.R. Pelaez-Samaniego, V. Yadama, T. Garcia-Perez, E. Lowell, T. Amidon, Effect of hot water extracted hardwood and softwood chips on particleboard properties, Holzforschung 68 (7) (2014) 807–815, http://dx.doi.org/10.1515/hf-2013-0150.

- [79] G. He, N. Yan, Effect of moisture content on curing kinetics of pMDI resin and wood mixtures, Int. J. Adhes. Adhes. 25 (5) (2005) 450–455, http://dx.doi.org/ 10.1016/j.ijadhadh.2004.12.002.
- [80] D.E. Kretschmann, F.P.L. (Us), Effect of various proportions of juvenile wood on laminated veneer lumber, Russell J. Bertrand Russell Arch. 521 (1993) http://www.fpl.fs.fed.us/documnts/fplrp/fplrp521.pdf.
- [81] R. Hernandez, D.W. Green, D.E. Kretschmann, S.P. Verrill, Improved Utilization of Small-Diameter Ponderosa Pine in Glulam Timber, Technical Report, 2005, p. 20, http://dx.doi.org/10.2737/FPL-RP-625, https://www.fs.usda.gov/treesearch/pubs/20976.
- [82] Z. Wang, M. Gong, Y.H. Chui, Mechanical properties of laminated strand lumber and hybrid cross-laminated timber, Constr. Build. Mater. 101 (November 2017) (2015) 622–627, http://dx.doi.org/10.1016/j.conbuildmat.2015.10.035.
- [83] Z. Wang, J. Zhou, M. Gong, Y.H. Chui, X. Lu, Evaluation of modulus of elasticity of laminated strand lumber by non-destructive evaluation technique, BioResources 11 (1) (2016) 626–633, http://dx.doi.org/10.15376/biores.11.1. 626-633.
- [84] S. Wang, H. Gu, T. Neimsuwan, Layer thickness swell and related properties of commercial OSB products: A comparative study, in: 37th International Wood Composite Materials Symposium, 2003, pp. 65–76.

- [85] R.G. Erikson, T. Gorman, D.W. Green, D. Graham, Mechanical grading of lumber sawn from small-diameter lodgepole pine, ponderosa pine, and grand fir trees from northern idaho, For. Prod. J. 50 (8909) (2000) 59–65.
- [86] R. Ringman, A. Pilgard, C. Brischke, K. Richter, Mode of action of brown rot decay resistance in modified wood: A review, Holzforschung 68 (2) (2014) 239–246, http://dx.doi.org/10.1515/hf-2013-0057.
- [87] J. Niederwestberg, J. Zhou, Y.H. Chui, Mechanical properties of innovative, multi-layer composite laminated panels, Buildings 8 (10) (2018) 1–13, http://dx.doi.org/10.3390/buildings8100142.
- [88] W.G. Davids, N. Willey, R. Lopez-Anido, S. Shaler, D. Gardner, R. Edgar, M. Tajvidi, Structural performance of hybrid SPFs-LSL cross-laminated timber panels, Constr. Build. Mater. 149 (2017) 156–163, http://dx.doi.org/10.1016/j.conbuildmat.2017.05.131.
- [89] Q. Zhou, M. Gong, Y.H. Chui, M. Mohammad, Measurement of rolling shear modulus and strength of cross laminated timber fabricated with black spruce, Constr. Build. Mater. 64 (2014) 379–386, http://dx.doi.org/10.1016/j.conbuildmat. 2014.04.039.